ISSN 2616-5775 Vol. 7, Issue 5: 190-198, DOI: 10.25236/AJCIS.2024.070525

SOC Estimation for Lithium-Ion Batteries Based on the AEKF-SVM Algorithm

Lei Zhang[1,*], Qianqian Song[2], Jie Li[3]

[1]School of Network Engineering, Wuhu Institute of Technology, Wuhu, 241000, China
[2]College of Computer Science, Chongqing University, Chongqing, 400044, China
[3]School of Information and Artificial Intelligence, Wuhu Institute of Technology, Wuhu, 241000, China
[*]Corresponding author: 101137@whit.edu.cn

Abstract: *In light of societal progress, energy has emerged as a critical concern, and new energy sources are poised to become the energy mainstream. Among these developments, lithium-ion batteries play a pivotal role in the new energy industry. Accurately estimating the State of Charge (SOC) of lithium-ion batteries is essential for the proper functioning of devices like electric vehicles. However, the SOC of lithium-ion batteries cannot be measured directly by instruments and can only be estimated by measurable variables. This paper proposes a new algorithm for accurate SOC estimation using a combination of adaptive extended Kalman filtering (AEKF) and support vector machine (SVM) algorithms, taking into account the characteristics of lithium-ion batteries. The AEKF algorithm was employed to estimate the State of Charge (SOC) under the Beijing Bus Dynamic Stress Test (BBDST) condition. By leveraging the adaptive noise covariance advantage of the AEKF algorithm, a model that is more fitting for the lithium-ion battery was obtained. Subsequently, the SOC for the Hybrid Pulse Power Characterization (HPPC) and Dynamic Stress Test (DST) conditions were predicted. Experimental results revealed that the SVM-AEKF algorithm, when used for SOC estimation, resulted in a maximum error of 0.037% under the HPPC condition, marking an improvement of 8.9% compared to the AEKF algorithm. Under the DST condition, the maximum error was 0.335%, indicating a 6.9% improvement over the AEKF algorithm. These results underscore the potential of the SVM-AEKF algorithm in accurately estimating SOC, thereby holding promise for practical applications.*

Keywords: *power lithium battery; Thevenin; state of charge; adaptive extended Kalman filter; support vector machine*

1. Introduction

With the development of society, the demand for fossil energy [1] is gradually rising, while the amount of fossil energy storage is significantly declining. Concurrently, global warming [2] and the emergence of various extreme weather [3] events have made the vigorous development of new energy sources our best solution to the energy problem. Lithium-ion batteries [4], as a primary focus of the new energy industry, offer advantages such as high energy density, lightweight, good cycling performance, low self-discharge rate, and no memory effect [5]. Consequently, lithium-ion batteries are widely used in automobiles and other applications. Therefor The estimation of the battery's state of charge (SOC) has always been an important research direction [6].

As the state of charge (SOC) of a lithium-ion battery cannot be measured directly by instruments, it can only be estimated indirectly by measuring the voltage[7,8], current [9], and temperature of the battery. Additionally, the SOC of lithium-ion batteries is influenced by temperature, charge and discharge rates[10], and the degree of battery aging[11], making SOC monitoring particularly challenging. Common methods for predicting SOC include the open-circuit voltage method[12,13,14], internal resistance method[15,16], ampere-hour integration method[17], and discharge test method.

The open-circuit voltage method is simple and practical, but its main disadvantage is that the battery must be left to rest, preventing real-time SOC monitoring. The discharge test method is applicable to a wide range of batteries and is simple and accurate, but it takes a long time to complete. The accuracy of SOC estimation using the ampere-hour integration method depends on the initial value, and the estimation error increases significantly over time.

To address these challenges, researchers have proposed the Kalman filter method [18,19,20]for SOC

ISSN 2616-5775 Vol. 7, Issue 5: 190-198, DOI: 10.25236/AJCIS.2024.070525

estimation. This method uses the state equation of the battery to obtain an accurate SOC value based on the principle of minimum mean squared error. However, due to the non-linear operating characteristics of most lithium-ion batteries, the extended Kalman filter (EKF) algorithm[21,22,23] was introduced. This algorithm applies a Taylor expansion to the Kalman algorithm, ignoring higher-order terms.

To overcome the slow convergence and low accuracy of the Kalman filter algorithm, researchers also developed the Unscented Kalman filter (UKF) algorithm[24,25]. For example, Meng [26] et al. employed a joint adaptive UKF algorithm and a Support Vector Machine (SVM) algorithm to estimate the SOC of lithium-ion batteries. The adaptive UKF algorithm adjusts the noise covariance during the estimation process, and the least-squares SVM algorithm reduces the impact of internal battery characteristics on the SOC. Experimental results show that this algorithm achieves an absolute error of less than 2%, demonstrating its feasibility.

In this paper, we use the first-order Thevenin model to estimate the SOC of lithium-ion batteries. We employ the Adaptive Extended Kalman Filter (AEKF) algorithm [27] to estimate the SOC and use the SVM algorithm[28] to correct the SOC estimated by the AEKF algorithm, resulting in a more accurate SOC estimation.

2. Mathematical analysis

2.1. SVM-AEKF algorithm

The SVM algorithm is developed based on the Vapnik-Chervonenkis (VC) dimensional theory of statistical learning and the principle of structural risk minimization, which are currently considered the best approaches for statistical estimation and prediction learning from small samples. The AEKF algorithm enhances the Extended Kalman Filter (EKF) by incorporating the Sage-Husa adaptive filtering method. This addition allows the statistical characteristics of noise in the filtering algorithm to be updated adaptively with changes in estimation results. To combine the advantages of both algorithms, the SVM-AEKF algorithm has been proposed in this paper.

The specific implementation steps of the algorithm are as follows: first, train a Support Vector Machine (SVM) model with three inputs and one output. The inputs are the voltage value Uk at time k, the State of Charge (SOC) estimate $s(k)$ from the Adaptive Extended Kalman Filter (AEKF) algorithm, and the predicted SOC value $\hat{s}(k)$ from the integration of the ampere-time. The output is the estimation error $s(k) - \hat{s}(k)$ of the AEKF algorithm. The SVM model uses the Radial Basis Function (RBF) kernel function. The flowchart of the SVM-AEKF algorithm is shown in Fig. 1.

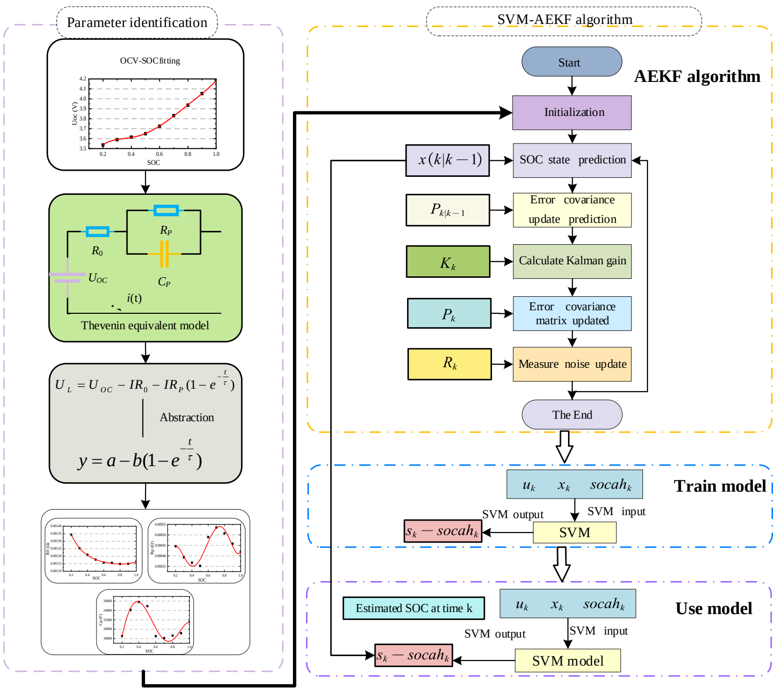

Figure 1: SVM-CKF algorithm flow chart Experimental analysis

ISSN 2616-5775 Vol. 7, Issue 5: 190-198, DOI: 10.25236/AJCIS.2024.070525

2.2. Equivalent modeling and Parameter identification

Modeling lithium-ion batteries is crucial for accurately estimating their State of Charge (SOC). These batteries undergo complex internal chemical reactions during charge and discharge cycles, making the selection of a suitable model essential for precise SOC estimation. Commonly utilized models include electrochemical models, data-driven models, and equivalent circuit models.

Electrochemical models, while accurate, suffer from high complexity, significant computational requirements, and a tendency to overfit, resulting in subpar SOC estimation accuracy. Data-driven models, such as neural network models, demand extensive experimental data for training and can be time-consuming and costly to develop, often requiring server resources.

Equivalent circuit models, such as the Rint model and the Thevenin model, offer a different approach by using standard circuit components to represent the battery's external characteristics. The Thevenin model, comprising a resistor and an RC circuit, effectively captures both the internal resistance and polarization of the lithium-ion battery. In contrast, the Rint model lacks the RC circuit and cannot fully depict the battery's internal polarization characteristics.

Given its advantages, this paper opts to model the lithium-ion battery using the Thevenin model, as illustrated in Fig. 2.

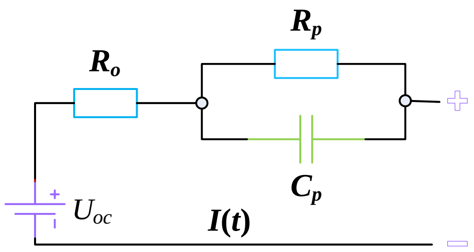

Figure 2: Thevenin equivalent circuit model

Fig. 2 shows the Thevenin model, where R_o is the ohmic internal resistance, R_p is the polarization resistor and C_p is the polarization capacitor in the RC circuit, U_p is the polarization voltage, U_{oc} is the open-circuit voltage, U_L is the terminal voltage, and U_0 is the voltage across the ohmic internal resistance. According to Kirchhoff's law in the circuit, the following expressions can be obtained from this model as shown in Eq. (1).

$$\begin{cases} U_L = E(t) - U_o - U_p \\ I(t) = C_p \dfrac{dU_p}{dt} + \dfrac{U_p}{R_p} \end{cases} \tag{1}$$

According to the definition of SOC: the ratio of the remaining capacity of a lithium-ion battery to the nominal capacity of the battery. The commonly used calculation method is the ampere-time integration method, whose equation is shown in Eq. (2).

$$SOC(t) = SOC(t_0) - \int_0^t \frac{\eta \cdot i(t)}{3600 \cdot C} dt \tag{2}$$

η represents the rated capacity of the battery and represents the current of charging and discharging the battery at time t. Since the open-circuit voltage is usually a function of the SOC of the lithium-ion battery, while using the knowledge of modern control theory, the equivalent circuit can be discretized to obtain a discretized model of the lithium-ion battery, whose state-space equations are shown Eq. (3).

$$\begin{cases} \begin{bmatrix} SOC_{k-1} \\ U_P \end{bmatrix} = \begin{bmatrix} 1 & 0 \\ 0 & e^{-\frac{\Delta t}{\tau_1}} \end{bmatrix} \begin{bmatrix} SOC_k \\ U_{0,k+1} \end{bmatrix} + \begin{bmatrix} -\frac{\Delta t}{Q_N} \\ R_p\left(1-e^{-\frac{T}{\tau}}\right) \end{bmatrix} I_k + \begin{bmatrix} w_{1,k} \\ w_{2,k} \end{bmatrix} \\ U_0 = U_{OC} - I_k R_{0,k} + \begin{bmatrix} 0 \\ -1 \end{bmatrix}^T \begin{bmatrix} SOC_k \\ U_{1,k} \end{bmatrix} + v_k \end{cases} \tag{3}$$

where Δt is the sampling interval, τ is the time constant, and its expression is $\tau_p = R_pC_p$, w is the state error, and v is the measurement error.

2.3. Parameter identification

Parameter identification involves determining the values of each parameter in a model based on existing experimental data and the established model. Common methods for parameter identification include offline and online parameter identification.

Offline parameter identification involves obtaining the OCV-SOC curves from HPPC conditions and then solving for the parameters of each component at different SOC values based on the relationships in the Thevenin model. The values of each component and SOC are then determined by least-squares polynomial fitting, which establishes the relationship between each component and SOC.Online parameter identification, on the other hand, uses the least-squares method to continuously correct and update the system's parameters, yielding more accurate identification results. However, due to its complexity and high computational demands, this paper employs the offline parameter identification method.

2.4. Adaptive extended Kalman algorithm

The adaptive Kalman filter algorithm is developed based on the extended Kalman filter algorithm, which achieves accurate estimation of the SOC of lithium-ion batteries by continuously updating the system noise and process noise based on the extended Kalman filter algorithm. The system needs to be initialized first, and the calculation process is shown in Eq. (4)

$$\begin{cases} \hat{X}_k = E\left(X_0\right) \\ P_k = E\left(X_0 - \hat{X}_k\right)\left(X_0 - \hat{X}_k\right)^T \end{cases} \tag{4}$$

where is the estimated value of the initial state and is the error covariance matrix. Then the update of the error covariance is performed, along with the Kalman gain, whose equation is shown in Eq. (5).

$$\begin{cases} \hat{P}_{k+1} = A_k P_k A_k{}^T + Q_k \\ K_{k+1} = \hat{P}_{k+1} C_{k+1}^T \left(C_{k+1} \hat{P}_{k+1} C_{k+1}^T + R_{k+1}\right)^{-1} \end{cases} \tag{5}$$

The Kalman gain coefficient is obtained, while combining the difference between the real-time observation data and the system observation data, the a priori estimate can be corrected, if the difference is large then the magnitude of the correction is also large, the difference is small the magnitude of the correction equation is shown in Eq. (6)

$$\begin{cases} x_{k+1} = \hat{x}_{k+1} + K_{k+1}(y_{k+1} - C_{k+1}\hat{x}_{k+1} - D_{k+1}u_{k+1}) \\ P_{k+1} = (E - K_{k+1}C_{k+1})\hat{P}_{k+1} \end{cases} \tag{6}$$

The adaptive regulation of SOC is achieved by estimating and correcting the statistical characteristics of the process noise and the measurement noise of the system with the following Eq. (7).

ISSN 2616-5775 Vol. 7, Issue 5: 190-198, DOI: 10.25236/AJCIS.2024.070525

$$\begin{cases} q_k = (1-d_{k-1})q_{k-1} + d_{k-1}G(\hat{x}_k - A\hat{x}_{k-1} - Bu_{k-1}) \\ Q_k = (1-d_{k-1})Q_{k-1} + d_{k-1}G(L_k \bar{y}_k \bar{y}_k^T L_k^T + P_k - AP_{k|k-1}A^T)G^T \\ r_k = (1-d_{k-1})r_{k-1} + d_{k-1}(y_k - C\hat{x}_{k|k-1} - Du_{k-1} - d) \\ R_k = (1-d_{k-1})R_{k-1} + d_{k-1}(\bar{y}_k \bar{y}_k^T - CP_{k|k-1}C^T) \end{cases} \tag{7}$$

2.5. Support Vector Machine algorithm

Support Vector Machines (SVM) are widely used in supervised learning for classification and regression tasks. The core idea behind SVM is to find the optimal hyperplane that separates different classes of data points by maximizing the margin between them. This approach enhances classification accuracy and generalization to new data. Support Vector Regression (SVR) is an extension of SVM used for regression analysis. Unlike classification, SVR aims to find a function that closely approximates the data points within a specified tolerance while controlling model complexity. SVR achieves this by adjusting the distance to the farthest data points, striking a balance between model bias and variance.

3. Experiment

3.1. Experimental result

The commonly used methods for offline parameter identification are the point-taking calculation method and the curve-fitting method. The point-taking calculation method uses only a few data points from the many data points of impulse response in the HPPC condition, discarding a large amount of data. This may lead to inaccurate data identification results, and the complex formulas involved are prone to errors during actual operation. Therefore, this paper adopts the curve-fitting method, which is simpler to execute and makes better use of the data points.

Firstly, a suitable line segment for curve fitting is selected. Using the Thevenin model, the expression of the circuit in the zero state can be derived, as shown in Eq. (8).

$$U_L = U_{oc} - IR_0 - IR_P(1 - e^{-\frac{x}{c}}) \tag{8}$$

The values of ohmic internal resistance R_0, polarized internal resistance R_p, and polarized capacitance C_p in the Thevenin model can be obtained by calculating the data using HPPC experiments, and the results are shown in Tab.1.

Table 1: Model parameters under different SOC states

SOC/100%	R_0/mΩ	R_p /mΩ	C_p /F	U_{oc}/V
0.1	1.961057682	0.519082	12519.57063	3.4592
0.2	1.859498063	0.390383	19667.75322	3.5410
0.3	1.825930538	0.350388	23038.81399	3.5897
0.4	1.802504690	0.319963	23332.61905	3.6166
0.5	1.780507248	0.344103	23954.96034	3.6514
0.6	1.758224125	0.524653	16215.69966	3.7360
0.7	1.745939839	0.523653	16879.77215	3.8318
0.8	1.730370221	0.482801	17187.37110	3.9350
0.9	1.723228194	0.435092	18133.44121	4.0497
1.0	1.718942978	0.426950	22069.80251	4.1840

To verify the performance of the first-order Thevenin model, the Thevenin model is constructed using Matlab, and the simulation results using the Thevenin model can be obtained by comparing the actual voltage with the simulated voltage, and the results are shown in Fig. 3

ISSN 2616-5775 Vol. 7, Issue 5: 190-198, DOI: 10.25236/AJCIS.2024.070525

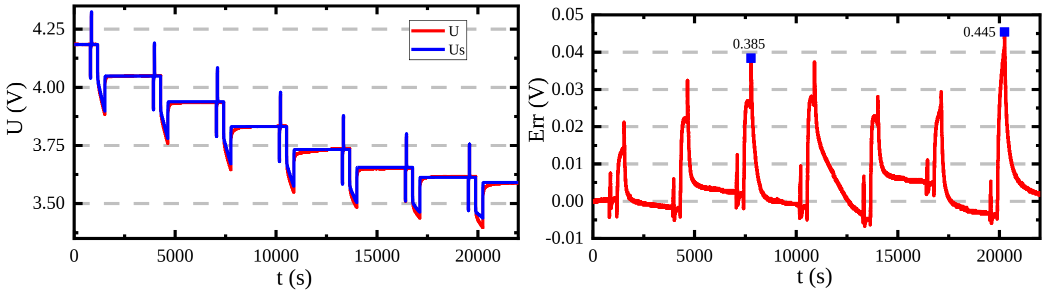

(a) Voltage Comparison Curve *(b) Simulation error*

Figure 3: Thevenin model simulation results

In the figure above, U represents the actual voltage, while Us represents the simulated voltage. Comparing the actual voltage with the simulated output in Fig. 3(a), it can be observed that the simulated output closely tracks the voltage changes of the Li-ion battery. From Fig. 3(b), it can be concluded that the maximum error is less than 0.05V, with an overall error maintained around 0.04V. When the SOC of the lithium-ion battery is at 0.1, the difference between the model output voltage and the actual voltage is relatively large, approximately 0.05V. However, this difference is small enough to be considered negligible.

3.2. Algorithm Comparison

To verify the accuracy of the algorithm, experiments are necessary. In this experiment, a ternary lithium-ion battery with a nominal capacity of 70Ah was used. After capacity testing, its capacity was measured to be 70.4Ah. The data from BBDST working conditions were selected to train the SVM model at a room temperature of 25℃, with SOC ranging from 1 to 0.1 and a sampling interval of 1s. The voltage variation under BBDST working conditions is illustrated in Fig. 5(a). The error results obtained by using the AEKF algorithm to predict the SOC for the BBDST condition are presented in Fig. 5(b).

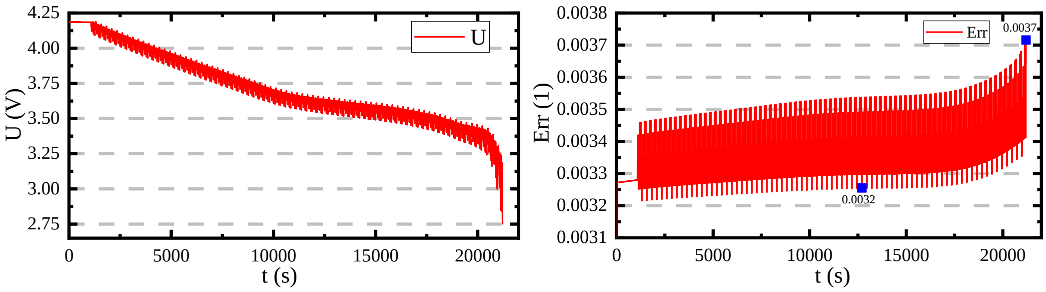

(a)BBDST Voltage Curve *(b) AEKF algorithm for estimating error curves*

Figure 4: AEKF-based lithium-ion battery SOC estimation effect

The maximum error in SOC estimation by the AEKF algorithm for the BBDST condition is 0.0037, indicating high accuracy. This result also validates the accuracy of the Thevenin model, as seen in Fig. 4(b). Consequently, the SOC of the BBDST condition obtained by the AEKF algorithm and the error between the predicted SOC and the true SOC are input into the SVM for training. The training data were divided into a 7:3 ratio, with 70% used as training data and 30% as validation data.

To demonstrate the proposed algorithm's adaptability to different operating conditions, the HPPC and DST operating conditions were selected for testing. These conditions simulate the lithium-ion battery's actual operating conditions as closely as possible. The SVM model was verified using these two operating conditions. The SOC estimation results and SOC errors for the HPPC operating condition are shown in Fig. 5.

ISSN 2616-5775 Vol. 7, Issue 5: 190-198, DOI: 10.25236/AJCIS.2024.070525

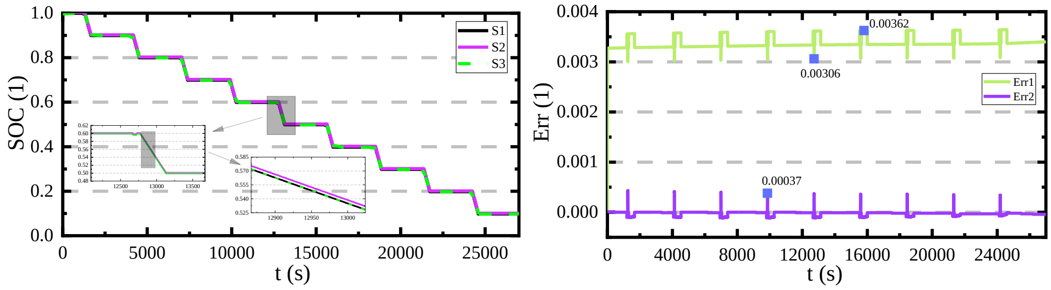

(a) SOC estimation in HPPC condition *(b) SOC estimation errors in HPPC condition*

Figure 5: SVM-AEKF-based lithium battery SOC estimation effect in BBDST condition

In Fig. 5(a), the SOC estimated by the AEKF algorithm and the SVM-AEKF algorithm is depicted. Here, S1 represents the SOC estimated by the ampere-time integration method, S2 represents the SOC predicted by the AEKF algorithm, and S3 represents the SOC predicted by the SVM-AEKF algorithm. Fig. 5(b) shows the SOC estimation errors, where Err1 represents the SOC estimation error of the AEKF algorithm, and Err2 indicates the SOC estimation error of the SVM-AEKF algorithm. Combining the two experimental result plots, it can be concluded that the maximum error of the SVM-AEKF algorithm proposed in this paper is 0.037%, while the maximum error of the AEKF algorithm is 0.362%. Therefore, it can be concluded that the SVM-AEKF algorithm has higher accuracy compared to the traditional AEKF algorithm.

The experimental data from DST conditions are once again utilized to validate the trained SVM model, with the validation results depicted in Fig. 6.

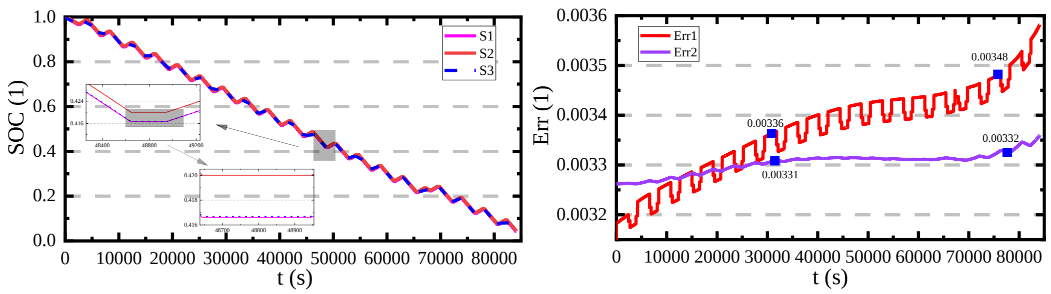

(a) SOC estimation in DST condition *(b) SOC estimation errors in DST condition*

Figure 6: SVM-AEKF-based lithium battery SOC estimation effect in DST condition

In Fig. 6(a), the SOC estimation results for the DST condition are plotted, where S1 represents the SOC estimated by the ampere-time integration method, S2 represents the SOC estimated by the AEKF algorithm, and S3 represents the SOC estimated by the SVM-AEKF algorithm. Fig. 6(b) shows the SOC estimation error, where Err1 is the error curve of the SOC estimated by the AEKF algorithm, and Err2 is the error curve of the SOC estimated by the SVM-AEKF algorithm. From the figure, it can be concluded that the maximum error of the AEKF algorithm is 0.360%, while the maximum error of the SVM-AEKF algorithm is approximately 0.335%. Additionally, the error fluctuation of the SVM-AEKF algorithm is significantly smaller than that of the AEKF algorithm.

4. Conclusions

With the dual pressures of resource scarcity and environmental concerns, lithium-ion batteries are becoming increasingly important as a clean energy source for future development. This paper proposes an SVM-AEKF algorithm using the Thevenin model with ternary Li-ion batteries as the research subject, aiming to predict the charge state of Li-ion batteries under different operating conditions. Experimental results demonstrate that the SVM-AEKF algorithm achieves a maximum error of only 0.037% under HPPC conditions and 0.335% under DST conditions, showing higher accuracy compared to the traditional AEKF algorithm. However, due to the limited availability of experimental data, this study does not consider the effect of temperature on SOC estimation. It is hoped that future research will address this aspect.

Acknowledgments

This research was supported by the 2024 Wuhu Institute of Technology Scientific Research Project (Project Number:[wzyzr202422]). We express our sincere gratitude for this support.

References

[1] Wang, W., L.W. Fan, and P. Zhou, Evolution of global fossil fuel trade dependencies. Energy, 2022. 238.
[2] Hu, X.M., et al., Inferring future warming in the Arctic from the observed global warming trend and CMIP6 simulations. Advances In Climate Change Research, 2021. 12(4): p. 499-507.
[3] Li, Z.H., et al., Knowledge map and global trends in extreme weather research from 1980 to 2019: a bibliometric analysis. Environmental Science And Pollution Research, 2021. 28(36): p. 49755-49773.
[4] Kulova, T.L., et al., A Brief Review of Post-Lithium-Ion Batteries. International Journal Of Electrochemical Science, 2020. 15(8): p. 7242-7259.
[5] Martins, L.S., et al., Electric car battery: An overview on global demand, recycling and future approaches towards sustainability. Journal Of Environmental Management, 2021. 295.
[6] Li, Z., et al., Review of lithium-ion battery state of charge estimation. Global Energy Interconnection, 2021. 4:p. 619-630
[7] Wang, P., et al., Temperature estimation from current and voltage measurements in lithium-ion battery systems. Journal Of Energy Storage, 2021. 34.
[8] Zhao, B., et al., Estimation of the SOC of Energy-Storage Lithium Batteries Based on the Voltage Increment. Ieee Access, 2020. 8: p. 198706-198713.
[9] Messing, M., et al., Low Temperature, Current Dependent Battery State Estimation Using Interacting Multiple Model Strategy. Ieee Access, 2021. 9: p. 99876-99889.
[10] Gao, T.F., et al., Hazardous characteristics of charge and discharge of lithium-ion batteries under adiabatic environment and hot environment. International Journal Of Heat And Mass Transfer, 2019. 141: p. 419-431.
[11] Jaguemont, J., et al. Low Temperature Aging Tests for Lithium-ion Batteries. in 24th IEEE International Symposium on Industrial Electronics (ISIE). 2015. Rio de Janeiro, BRAZIL.
[12] Gismero, A., E. Schaltz, and D.I. Stroe, Recursive State of Charge and State of Health Estimation Method for Lithium-Ion Batteries Based on Coulomb Counting and Open Circuit Voltage. Energies, 2020. 13(7).
[13] Zhang, Q., et al., Fractional calculus based modeling of open circuit voltage of lithium-ion batteries for electric vehicles. Journal Of Energy Storage, 2020. 27.
[14] Yu, Q.Q., et al., An Open Circuit Voltage Model Fusion Method for State of Charge Estimation of Lithium-Ion Batteries. Energies, 2021. 14(7).
[15] Sun, L., G.R. Li, and F.Q. You, Combined internal resistance and state-of-charge estimation of lithium-ion battery based on extended state observer. Renewable & Sustainable Energy Reviews, 2020. 131.
[16] Chen, L., et al., Estimation the internal resistance of lithium-ion-battery using a multi-factor dynamic internal resistance model with an error compensation strategy. Energy Reports, 2021. 7: p. 3050-3059.
[17] Li, H.H., et al., State of Charge Estimation for Lithium-Ion Battery Models Based on a Thermoelectric Coupling Model. International Journal of Electrochemical Science, 2020. 15(5): p. 3807-3824.
[18] Yan, Q.C., et al., State of Charge Estimation for Lithium-Ion Battery via MILS Algorithm Based on Ensemble Kalman Filter. International Journal of Photoenergy, 2021. 2021.
[19] Thenaisie, G., C.H. Park, and S.G. Lee, A Real-Time Entropy Estimation Algorithm for Lithium Batteries Based on a Combination of Kalman Filter and Nonlinear Observer. Ieee Transactions on Industrial Electronics, 2020. 67(9): p. 8034-8043.
[20] Li, Y., et al., Constrained Ensemble Kalman Filter for Distributed Electrochemical State Estimation of Lithium-Ion Batteries. Ieee Transactions on Industrial Informatics, 2021. 17(1): p. 240-250.
[21] Jiang, C., et al., A state-of-charge estimation method of the power lithium-ion battery in complex conditions based on adaptive square root extended Kalman filter. Energy, 2021. 219.
[22] Imran, R.M., Q. Li, and F.M.F. Flaih, An Enhanced Lithium-Ion Battery Model for Estimating the State of Charge and Degraded Capacity Using an Optimized Extended Kalman Filter. Ieee Access, 2020. 8: p. 208322-208336.
[23] Li, W.Q., et al., The multi-innovation extended Kalman filter algorithm for battery SOC estimation.

ISSN 2616-5775 Vol. 7, Issue 5: 190-198, DOI: 10.25236/AJCIS.2024.070525

Ionics, 2020. 26(12): p. 6145-6156.
[24] Huang, M.T., et al., Quadrature Kalman filter-based state of charge estimation for lithium-ion battery. Advances In Mechanical Engineering, 2020. 12(7).
[25] Wang, K., et al., State of Charge (SOC) Estimation of Lithium-ion Battery Based on Adaptive Square Root Unscented Kalman Filter. International Journal Of Electrochemical Science, 2020. 15(9): p. 9499-9516.
[26] Meng, J.H., G.Z. Luo, and F. Gao, Lithium Polymer Battery State-of-Charge Estimation Based on Adaptive Unscented Kalman Filter and Support Vector Machine. Ieee Transactions on Power Electronics, 2016. 31(3): p. 2226-2238.
[27] Zhu, Q., et al., A state of charge estimation method for lithium-ion batteries based on fractional order adaptive extended kalman filter. Energy, 2019. 187.
[28] Li, R., et al., State of Charge Prediction Algorithm of Lithium-Ion Battery Based on PSO-SVR Cross Validation. Ieee Access, 2020. 8: p. 10234-10242.